Benefits of Co-Locating Concentrating Solar Power and Wind

Ramteen Sioshansi, *Senior Member, IEEE* and Paul Denholm, *Senior Member, IEEE*

***Abstract*—We analyze the potential benefits of co-locating wind and concentrating solar power (CSP) plants in the southwestern U.S. Using a location in western Texas as a case study, we demonstrate that such a deployment strategy can improve the capacity factor of the combined plant and the associated transmission investment. This is because of two synergies between wind and CSP: (i) the negative correlation between real-time wind and solar resource availability and (ii) the use of low-cost high-efficiency thermal energy storage in CSP. The economic tradeoff between transmission and system performance is highly sensitive to CSP and transmission costs. We demonstrate that a number of deployment configurations, which include up to 67% CSP, yield a positive net return on investment.**

***Index Terms*—Concentrating solar power, wind, thermal energy storage, transmission**

NOMENCLATURE

A. Optimization Model Sets and Parameters

T	set of hours in optimization horizon
C	set of concentrating solar power (CSP) plants
κ	transmission capacity
λ	transmission losses
p_c^s	charging capacity of thermal energy storage (TES) system of CSP plant c
p_c^d	discharge capacity of TES system of CSP plant c
h_c	hours of storage in TES system of CSP plant c
η_c	hourly energy retention of TES system of CSP plant c
ρ_c	roundtrip efficiency losses of CSP plant c
e_c^-	minimum power capacity of powerblock of CSP plant c
e_c^+	maximum power capacity of powerblock of CSP plant c
$f_c(\cdot)$	heat rate function of powerblock of CSP plant c
$g_c^H(\cdot)$	HTF pump parasitics function of CSP plant c
$g_c^B(\cdot)$	balance of plant parasitics function of CSP plant c
e_c^{SU}	startup energy of powerblock of CSP plant c
μ_c	minimum up-time of powerblock of CSP plant c
α_c	variable cost of CSP plant c
π_t	price of energy in hour t
$e_{c,t}^{SF}$	thermal energy collected by solar field of CSP plant c in hour t
$\bar{w}_t$	total wind energy available in hour t
γ	wind production tax credit (PTC)

This work was supported by the U.S. Department of Energy through prime contract DE-AC36-08GO28308 and by the Alliance for Sustainable Energy, LLC through subcontract AGG-0-40365-01.

R. Sioshansi is with the Integrated Systems Engineering Department, The Ohio State University, Columbus, OH 43210, USA (e-mail: sioshansi.1@osu.edu).

P. Denholm is with the Strategic Energy Analysis Center, National Renewable Energy Laboratory, Golden, CO 80401, USA (e-mail: paul.denholm@nrel.gov).

B. Optimization Model Decision Variables

$l_{c,t}$	storage level of TES of CSP plant c at the end of hour t
$s_{c,t}$	energy stored by TES of CSP plant c in hour t
$d_{c,t}$	energy discharged from TES of CSP plant c in hour t
$\sigma_{c,t}$	binary variable that equals 1 if TES of CSP plant c is being charged in hour t
$e_{c,t}^{PB}$	thermal energy delivered to powerblock of CSP plant c in hour t
$e_{c,t}^{net}$	net generation from CSP plant c in hour t
$u_{c,t}$	binary variable that equals 1 if powerblock of CSP plant c is online in hour t
$r_{c,t}$	binary variable that equals 1 if powerblock of CSP plant c is started up in hour t
w_t	wind generated in hour t
n_t^s	gross electric energy sold in hour t
n_t^p	gross electric energy purchased in hour t
n_t	binary variable that equals 1 if energy is being sold in hour t

C. Capacity Value Parameters and Variables

$\tilde{T}$	subset of hours with highest loads
$\tilde{e}_{c,t}^{PB}$	maximum thermal energy that can be delivered to powerblock of CSP plant c in hour t
$\tilde{d}_{c,t}$	amount of $\tilde{e}_{c,t}^{PB}$ that is taken from TES of CSP plant c in hour t
$\tilde{e}_{c,t}^{net}$	maximum potential output of CSP plant c in hour t
$\tilde{n}_t^s$	maximum potential net generation from deployment in hour t
Λ_t	loss of load probability (LOLP) in hour t
ξ_t	LOLP-based weight in hour t

D. Return on Investment Parameters and Variables

χ^e	annual net energy revenues
χ^c	annual capacity revenues
χ^p	annual PTC revenues
ψ^w	total wind capital cost
ψ^s	total CSP capital cost
ψ^t	total transmission capital cost
Υ^{ITC}	CSP investment tax credit

I. INTRODUCTION

A challenge in deploying renewables is the often remote location of high-quality wind and solar resources, requiring new transmission. The state of Texas was one of the first regions of the U.S. to contend with this issue. The highest quality wind is located in the western part of the state, while the major population centers are in the east. About 1.4 GW of

wind was added in the McCamey region of Texas in 2001 and 2002, despite there only being about 400 MW of transmission capacity [1]. This resulted in about 380 GWh of wind being curtailed in 2002 at an estimated cost of more than $21.4 million. Although transmission capacity has since been added, this construction has not kept pace with wind development. Wind curtailment in the Electric Reliability Council of Texas (ERCOT) was about 9% in 2011 [2].

New transmission is often difficult to construct and, if only carrying wind, lightly loaded. This is due to wind's low capacity factor, which is typically less than than 40%. One option to increase transmission utilization is to co-locate wind with other resources that can complement its generation. Denholm and Sioshansi [3] model co-located wind and compressed-air energy storage, showing good synergies between the two. Another option, in some parts of the world, is to co-locate wind with concentrating solar power (CSP). West Texas has good wind resources that are close to locations with sufficient direct normal irradiance (DNI) for economic siting of CSP. Fig. 1 illustrates this by overlaying areas of Texas that have at least class-4 wind (an average wind speed of at least 7 m/s at a 50 m height) and an average daily DNI of at least 5 kWh/m^2. Fig. 1 excludes areas that are unsuitable for development, by filtering out environmentally sensitive lands, urban areas, water features, terrain with more than a 3% average land slope, and areas with less than 1 km^2 of contiguous land space.

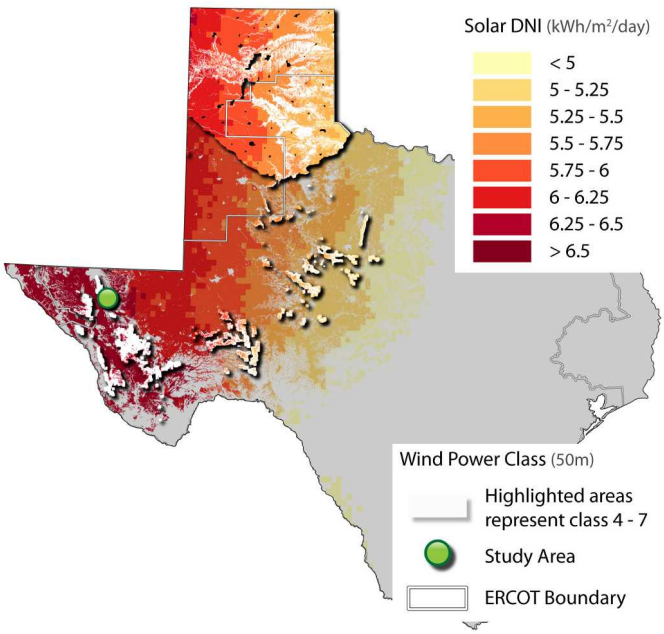

Fig. 1. Average DNI of locations in Texas with at least class-4 wind.

CSP plants have an additional advantage of being able to incorporate low-cost and high-efficiency thermal energy storage (TES), making them partially dispatchable [4]–[11]. While CSP has yet to be developed in Texas, the prospect of decreasing costs could result in future deployments [12], [13]. CSP in ERCOT faces the same challenges as wind in requiring new transmission from western to eastern Texas. However, CSP has the opportunity to use transmission built primarily for wind. Due to the relatively low capacity factor of wind and the dispatchability of CSP with TES, CSP could 'fill in' during periods of low wind output.

This sharing of transmission does present some limitations, however. To maximize transmission utilization, total transmission capacity is less than the maximum output of the CSP and wind plants. Ideally, CSP is dispatched to provide maximum output during highest-priced periods. The CSP plant may, however, be forced to shift output to lower-priced periods due to transmission constraints. In addition, there can be extended periods of high wind and solar output, resulting in curtailed generation. Thus, co-location of wind and CSP represents a tradeoff between maximizing the value of energy produced and the transmission costs.

In this paper we examine this tradeoff and identify opportunities for co-location of wind and CSP. We develop a model that optimizes the dispatch of co-located wind and CSP plants. Using historical ERCOT market and weather data, we examine the effect of different deployment configurations that are connected to the grid by a radial transmission line. We further demonstrate that a number of deployment configurations, which include up 67% CSP, yield a positive net year-1 return on investment (ROI). This analysis expands upon the work of Denholm and Sioshansi [3], in that we study all-renewable deployments sharing transmission resources. We also demonstrate important synergies between wind and CSP, including negative correlation of their real-time availability and the added flexibility that TES offers. The remainder of this paper is organized as follows: Section II discusses the models, case study, and data used in our analysis, Section III summarizes our results, and Section IV concludes.

II. Model and Case Study

We base our analysis on the CSP optimization model that Sioshansi and Denholm [12] develop. The model takes the characteristics of the combined plant (*e.g.* number and configuration of CSP plants and wind and transmission capacities), weather, and market price data as fixed, and optimizes deployment dispatch to maximize revenues. We model deployments at the location shown in Fig. 1, which is at coordinates 31.49° N, 104.56° W. The deployments are assumed to be connected to the Dallas area by a radial transmission line. The linear distance from the deployment to the connection point is 931 km. We assume the length of the transmission line is 12% greater than this linear distance and 4.9% transmission losses, based on the characteristics of the Intermountain Power Project from Utah to southern California [14]. The location is not optimized, but is a site with good wind and CSP resources. We examine generator dispatch and resulting revenues during the years 2004 and 2005, for which high-resolution wind and solar resource data are available.

A CSP plant consists of three interrelated components that can be sized differently. The first is the solar field, which is a field of mirrors that concentrates solar radiation onto a heat transfer fluid (HTF). The second is the powerblock, which is a heat engine that converts thermal energy into electricity. The third is the TES system, which can store energy collected by

the solar field for later use in the powerblock. The size of the powerblock is measured by its rated output capacity, measured in MW-e. The size of the solar field can be measured by its solar multiple (SM). A solar field with a 1.0 SM is sized to provide sufficient thermal energy to operate the powerblock at its rated capacity with 950 W/m^2 DNI, 5 m/s wind speed, and 25° C ambient temperature. The solar field size scales relative to a field with a 1.0 SM (*e.g.*, a field with a 1.7 SM is 70% larger). The TES system has power and energy capacities. The power capacity, measured in MW-t, is the maximum rate at which energy can be charged and discharged. We assume that the charging capacity is scaled in proportion to the SM, so that the full output of the solar field can be stored if necessary. This is different from some designs using indirect TES, in which the heat exchanger used to transfer energy between the HTF and the TES fluid is sized to only exchange energy that exceeds the powerblock capacity. The energy capacity is typically measured by the number of hours of storage. We use this convention, defining it as the number of hours that TES can be discharged at its maximum rated power capacity.

Sizing these components is nontrivial since their relative sizes determine the capacity factor and utilization of a CSP plant. A smaller solar field typically results in many (daytime) hours during which the powerblock is not fully utilized. As the solar field size increases, powerblock utilization rises during these hours. There may, however, be other hours during which the thermal energy collected by the solar field would overload the powerblock and excess energy must go unused. Introducing TES to the CSP plant can help alleviate this issue, by storing excess energy during such hours, and this is one of the benefits of TES. Sioshansi and Denholm [12] and Madaeni *et al.* [13] further discuss these benefits of and issues in CSP plant design.

A. Wind and CSP Optimization Model

Our optimization model consists of two parts. The first uses the Solar Advisor Model (SAM) [15]. SAM is a software package, based on TRNSYS [16], that simulates CSP plant dynamics. SAM has been validated against empirical CSP operational data from the Solar Energy Generating Systems [17]. Weather data and CSP plant characteristics are input to SAM to determine how much thermal energy is collected by the solar field in each hour.

The second part of our model is a mixed-integer program (MIP) that optimizes deployment dispatch to maximize revenues. This model takes hourly thermal energy collected by the solar field, potential wind generation, and energy prices as inputs. The MIP formulation is given by:

$$\max \quad \sum_{t\in T}\left(\pi_t\cdot(n_t^s-n_t^p)+\gamma w_t-\sum_{c\in C}\alpha_c e_{c,t}^{net}\right); \tag{1}$$

$$\text{s.t.} \quad \frac{n_t^s}{1-\lambda}-(1-\lambda)n_t^p=w_t+\sum_{c\in C}e_{c,t}^{net}, \qquad \forall\, t\in T; \tag{2}$$

$$-\kappa\le\frac{n_t^s}{1-\lambda}-(1-\lambda)\cdot n_t^p\le\kappa, \qquad \forall\, t\in T; \tag{3}$$

$$0\le n_t^s\le\kappa\cdot n_t, \qquad \forall\, t\in T; \tag{4}$$

$$0\le n_t^p\le\kappa\cdot(1-n_t), \qquad \forall\, t\in T; \tag{5}$$

$$l_{c,t}=\eta_c\cdot l_{c,t-1}+s_{c,t}-d_{c,t}, \qquad \forall\, c\in C, t\in T; \tag{6}$$

$$0\le l_{c,t}\le h_c\cdot p_c^s, \qquad \forall\, c\in C, t\in T; \tag{7}$$

$$0\le s_{c,t}\le\sigma_{c,t}\cdot\min\{e_{c,t}^{SF},p_c^s\}, \qquad \forall\, c\in C, t\in T; \tag{8}$$

$$0\le d_{c,t}\le(1-\sigma_{c,t})\cdot p_c^d, \qquad \forall\, c\in C, t\in T; \tag{9}$$

$$1-u_{c,t}\le\sigma_{c,t}, \qquad \forall\, c\in C, t\in T; \tag{10}$$

$$s_{c,t}-\rho_c\cdot d_{c,t}+e_{c,t}^{PB}+e_c^{SU}\cdot r_{c,t}\le e_{c,t}^{SF}, \qquad \forall\, c\in C, t\in T; \tag{11}$$

$$e_{c,t}^{net}=f_c(e_{c,t}^{PB})-g_c^H(d_{c,t})-g_c^B(f_c(e_{c,t}^{PB})), \qquad \forall\, c\in C, t\in T; \tag{12}$$

$$e_c^-\cdot(u_{c,t}-r_{c,t})\le e_{c,t}^{PB}\le e_c^+\cdot(u_{c,t}-r_{c,t}), \qquad \forall\, c\in C, t\in T; \tag{13}$$

$$u_{c,t}-u_{c,t-1}\le r_{c,t}, \qquad \forall\, c\in C, t\in T; \tag{14}$$

$$\sum_{\tau=t-\mu_c}^{t}r_{c,\tau}\le u_{c,t}, \qquad \forall\, c\in C, t\in T; \tag{15}$$

$$\sigma_{c,t},u_{c,t},r_{c,t},n_t\in\{0,1\}, \qquad \forall\, c\in C, t\in T; \tag{16}$$

$$0\le w_t\le\bar{w}_t, \qquad \forall\, t\in T \tag{17}$$

Objective function (1) maximizes revenues from net energy sales and the wind production tax credit (PTC), net of variable CSP generation costs. Constraints (2) define net energy sales and purchases in terms of wind and CSP generation. Constraints (3) impose the transmission limit, and constraints (4) and (5) allow the deployment to only sell or purchase energy at any given time. Energy purchases only occurs when the CSP plants' parasitic loads are greater than gross CSP and wind generation, resulting in negative net deployment generation.

Constraints (6) define the amount of energy stored in the TES systems as a function of the previous storage level, plus any net energy charged. Constraints (7) impose the energy limits on the TES systems, and constraints (8) and (9) the charging and discharging power limits. They also prevent a TES system from charging and discharging energy simultaneously. Constraints (10) allow TES to be discharged only when the powerblock is online.

Constraints (11) limit net thermal energy used by each CSP plant to be no more than the amount collected by its solar field. Constraints (12) define net generation of the CSP plants based on the heat rate function and parasitic loads. Constraints (13) impose upper and lower operating bounds when the powerblocks are online. They also assume that the powerblocks take an hour to startup, during which time they do not produce energy. Constraints (14) define powerblock startups in terms of intertemporal changes in the $u_{c,t}$ variables and constraints (15) impose the minimum up-time requirement when powerblocks are started up. Constraints (16) impose integrality conditions and constraints (17) restrict wind generation to be less than that available.

B. Capacity Value Estimation

In addition to energy revenues, which are given by the optimized value of (1), we assume that the deployment receives capacity payments. These are supplemental payments made to a generator for the capacity that it provides the system. This payment is assumed to be the product of a fixed capacity price and the deployment's capacity value.

The literature proposes several capacity value estimation techniques for wind [18]–[22] and CSP [23], [24]. This includes reliability-based methods and approximations. One of the challenges in estimating the capacity value of CSP is that one must account for both how much energy the plant plans to produce and how much is in TES. This is because even if the plant plans not to generate electricity, energy in TES could be used in real-time to help avert a system capacity shortage.

We apply the technique proposed by Madaeni *et al*. [24] to the optimized operation of the deployment, as given by the MIP, to estimate the capacity value. This method determines the maximum amount of energy that could potentially be produced if all wind, solar field, and TES energy are used. We do this by first computing how much thermal energy could be delivered to each CSP powerblock in each hour as:

$$\begin{aligned}\tilde{e}^{PB}_{c,t} \quad = \quad & \max\left\{0, \min\left\{e^{+}_{c}, e^{SF}_{c,t}\right.\right. \\ & -e^{SU}_{c}\cdot(1+r_{c,t}-u_{c,t}) \\ & \left.\left.+\eta_c\cdot\min\left\{p^{d}_{c}, \rho_c\cdot l_{c,t-1}\right\}\right\}\right\}. \end{aligned} \tag{18}$$

Equation (18) defines $\tilde{e}^{PB}_{c,t}$ as the minimum of the rated powerblock capacity and the sum of energy collected by the solar field and in TES. It further assumes that the powerblock can be started up immediately (using the required thermal energy) in the event of a system shortage event. We next define the amount of this energy that is taken from TES as:

$$\tilde{d}_{c,t} = \max\{0, \tilde{e}^{PB}_{c,t} - e^{SF}_{c,t}\}. \tag{19}$$

The maximum potential output of each CSP plant is then defined as:

$$\tilde{e}^{net}_{c,t} = f_c(\tilde{e}^{PB}_{c,t}) - g^{H}_{c}(\tilde{d}_{c,t}) - g^{B}_{c}(f_c(\tilde{e}^{PB}_{c,t})). \tag{20}$$

We finally compute the maximum potential generation of the deployment as:

$$\tilde{n}^{s}_{t} = \min\left\{\kappa, \sum_{c\in C}\tilde{e}^{net}_{c,t} + \bar{w}_t.\right\} \tag{21}$$

We use the quantities, $\tilde{n}^{s}_{t}$, to estimate the capacity value of the deployment using a capacity factor-based approximation. Studies of wind and CSP show that considering the hours of the year with the highest loads and weighting the outputs of the plant by the system's loss of load probabilities (LOLPs) [25] provides the most robust capacity value estimate [18], [23], [24]. In the case of wind, using the 10% of the hours of the year with the highest loads provides the best estimate, whereas using the top-10 hours provides the best estimate for a CSP plant. As we consider a mix of wind and CSP, we opt to use the 10% of the hours with the highest loads.

To compute the capacity value, we define $\tilde{T} \subseteq T$ as the subset of hours considered in the approximation. We then define the weight in each of these hours as:

$$\xi_t = \frac{\Lambda_t}{\sum\limits_{\zeta\in\tilde{T}}\Lambda_\zeta}, \ \forall\ t \in \tilde{T}, \tag{22}$$

which then gives the following capacity value estimate:

$$\sum_{t\in\tilde{T}}\xi_t\cdot\tilde{n}^{s}_{t}. \tag{23}$$

C. Case Study

Our case study requires assumptions regarding the performance and characteristics of the CSP plant and the deployments, weather and price data for the optimization model, and system data to compute LOLPs and capacity values.

1) CSP Characteristics: We assume that the CSP plants modeled have the same characteristics as the default parabolic trough system in SAM version 2.0. This plant has a powerblock with a gross rated capacity of 110 MW-e, but can be run at 115% of this rated capacity. When the parasitic loads are taken into the account, the maximum net capacity of the plant is about 120 MW-e. The powerblock has a 25% minimum load requirement when online, consumes 29 MWh-t of energy to startup, and must remain online a minimum of one hour when started up. The plant includes a two-tank TES system, which we assume to have a roundtrip efficiency of 98.5% and hourly heat losses of 0.031% of the energy in storage [4], [5]. The 98.5% roundtrip efficiency does not account for potential exergy losses. Direct TES systems, such as those in some power tower designs, can minimize any such losses. We assume that the CSP plants have a 2.0 SM and four hours of TES, based on baseline plant designs in the CSP literature [10], but consider the benefits of more flexible designs in Section III-B. The TES charging capacity is 576 MW-t, which is the maximum potential power output of the solar field. We further assume variable generation costs to be \$0.70/MWh-e [15].

2) Deployment Characteristics: We assume a 1080 MW-e maximum deployment generating capacity and consider cases in which there are between zero and nine CSP plants. Wind generators are added to bring the nameplate capacity of the deployment to 1080 MW-e. For instance, a deployment with four CSP plants has 480 MW-e of CSP capacity and 600 MW of wind. We model cases in which the transmission line connecting the deployment to the load center has a capacity of between 600 MW and 1080 MW.

3) Weather and Resource Data: Weather data are obtained from the National Solar Radiation Data Base, which accounts for the effects of cloud cover and other variables on DNI [26]. Wind data are obtained from the National Renewable Energy Laboratory's Western Wind Resource Dataset [27]. This dataset converts modeled wind speeds into wind generation, thus no further modeling on our part is needed. We assume the wind is dispersed among 56 sites around the study location, each of which can accommodate up to 30 MW of wind.

4) Price Data: Balancing energy service prices for the ERCOT North Zone are obtained from the market operator.

5) Optimization Model: We optimize deployment operations using a rolling 24-hour planning horizon. This process works by starting at the beginning of the study period and optimizing the dispatch over a 48-hour period. The optimized dispatch for the first 24 hours is fixed and the process rolls forward to the second day. We use the 48-hour optimization horizon to ensure that energy is stored if it has value on the following day [28]. Our optimization model assumes that the generator has perfect foresight of weather and prices. Relaxing these assumptions has a limited effect on the profit and operation of a standalone CSP plant [12]. Co-located wind and CSP are likely more affected by such uncertainty, however.

6) Capacity Value Calculation: We compute system LOLPs using load data from the ERCOT market operator and generator data from Form 860 data collected by the U.S. Department of Energy's Energy Information Administration. These data specify the nameplate capacity and generating technology of each conventional plant. These are combined with historical effective forced outage rate data from the North American Electric Reliability Corporation's Generating Availability Data System to compute system LOLPs using a standard binary state model (*i.e.*, each generator is either on- or off-line in each hour), in which outages are serially and jointly independent.

We set the capacity price based on the capital cost of a natural gas-fired combustion turbine, which is estimated at $625/kW in 2005 dollars [29]. We use a combustion turbine since this is a generation technology often used for peak-capacity purposes. We use an 11% capital charge rate (CCR) [3] to convert this into an annual cost of $68.75/kW-year. The CCR accounts for financing and other parameters and converts the total capital cost into an annual cost.

III. Results

A. Dispatch of Wind and CSP Deployments

Wind and CSP have two complementarities that enable them to share transmission. One is that real-time wind and solar resource can be negatively correlated. The other is that CSP with TES is partially dispatchable, allowing solar to be shifted and to fill-in excess transmission capacity during lower-resource hours. Fig. 2 illustrates these complementarities by showing the dispatch of a deployment consisting of 480 MW-e of CSP, 600 MW of wind, and 600 MW of transmission over a two-day period beginning on 16 May, 2004. Since transmission is sized at the nameplate wind capacity, maximum deployment output is 180% of the transmission capacity. These days show some negative correlation between wind and solar resource—wind is relatively high overnight when there is no solar and the solar peak lags the midday wind peak by at least two hours. Thus, adding CSP allows for greater transmission usage.

Fig. 2 also demonstrates the other complementarity between wind and CSP—TES stores energy that would otherwise be curtailed. Roughly 32% of the energy collected by the solar fields is stored and used to produce energy later in the day. Despite this, about 21% of collected solar energy is wasted due to the limited energy capacity of the system. The figure shows these curtailments, which are defined as the differences between the left- and right-hand sides of constraints (11) and

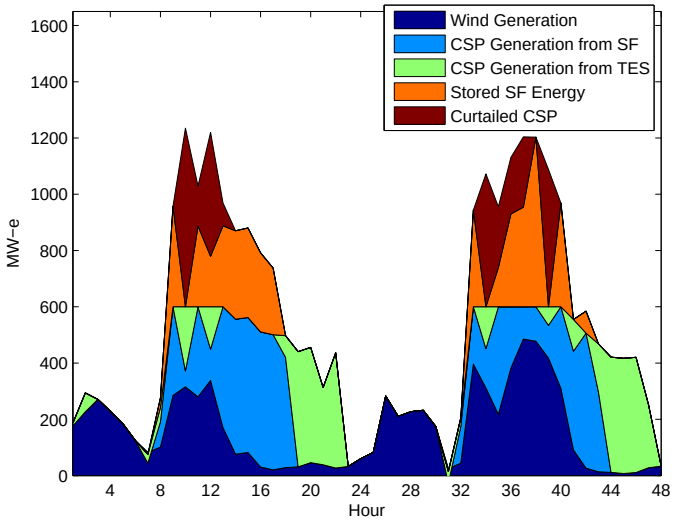

Fig. 2. Wind and CSP dispatch beginning 16 May, 2004.

represent thermal energy that the CSP plants' solar fields collect but goes unused. These curtailments are converted to MWh-e by applying the CSP plants' average net efficiency, accounting for parasitic loads. Despite this limitation, four hours of TES is able to reduce CSP curtailment by roughly 62% compared to no-TES plants.

There are limitations to these complementarities between CSP and wind. Some periods, which tend to occur in the spring, have extended high wind generation, during which the TES systems fill and limited transmission forces solar curtailment. Fig. 3 demonstrates this for the same deployment in Fig. 2 over a two-day period beginning on 22 April, 2004. About 71% of solar energy collected during this period is curtailed and annual curtailment is about 15%. Fig. 2 and 3 also show that the model prioritizes wind over CSP. This is both due to the wind PTC, which makes wind generation more valuable than CSP, and the higher variable cost of CSP. Our model only includes the $19/MWh (in 2005) Federal wind PTC. Other state and local incentives could provide wind with a further revenue advantage. Conversely, incentives for CSP could reduce the relative advantage of wind. However, this prioritization occurs unless any such incentives are equal for the two technologies, pointing to a distortion created by the different subsidies available for wind and solar.

Another limitation of having a downsized transmission link is that the CSP plant is dispatched 'around' wind generation and is operated in a suboptimal manner compared to a transmission-unconstrained deployment. This is illustrated in Fig. 4, which shows the optimized dispatch of a deployment with 480 MW-e of CSP and 600 MW-e of wind during a three-day period beginning on 17 October, 2004. Fig. 4a shows the operation of a transmission-unconstrained deployment. It shows that TES allows solar to be sold during the highest-priced hours, for instance in hours 18, 30, and 62 when prices are relatively high. Fig. 4b shows the operation of the deployment on the same days with 700 MW of transmission. It demonstrates the benefit of TES in allowing solar to be shifted to lower-resource hours. For instance, excess energy

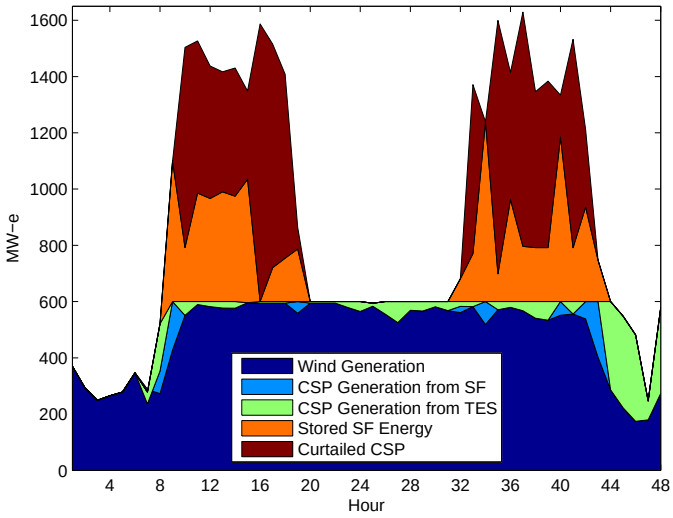

Fig. 3. Wind and CSP dispatch beginning 22 April, 2004.

that would overload transmission in hours 9 through 15 is stored and discharged in hours 16 through 21 and 28 through 33, with similar behavior on the following days. However, this dispatch of the CSP plant is suboptimal from a market value standpoint. This is because the transmission constraint does not allow the CSP plant to sell as much energy during hours 30 through 33, when prices are relatively high. It must, instead, sell this energy in hours 42 through 49. During the days shown in Fig. 4 the average selling price of CSP energy is $89.10/MWh-e in the transmission-unconstrained case, as opposed to only $71.05/MWh-e with the constraint. Denholm and Sioshansi [3] demonstrate the same phenomenon when storage is co-located with a transmission-constrained wind generator. These operational policies and the resulting revenue differences represent a tradeoff between the cost and challenges of transmission development versus the optimal dispatch of CSP and TES.

Fig. 2 through 4 point to the tradeoffs in co-locating wind and CSP. Downsizing transmission increases the capacity factor, but also increases generator curtailment and decreases the value of the energy produced. Fig. 5 through 7 illustrate these tradeoffs by showing average annual transmission capacity factors, curtailments, and energy revenues for different deployment configurations. Thermal energy that is unused by the CSP plants is converted to MWh-e, using the average plant efficiency, to estimate total energy curtailment in Fig. 6. The wind generators modeled have capacity factors of about 33.9%, as opposed to 34.5% for the CSP plants. Thus, if the deployment is transmission-unconstrained, a CSP-only mix maximizes transmission capacity factor. Otherwise, it is beneficial to build a mix of wind and CSP to exploit negative resource correlation. With 600 MW and 800 MW of transmission 480 MW-e and 600 MW-e of CSP maximize the transmission capacity factor at 57% and 45%, respectively.

CSP generation is curtailed in all cases modeled, including a transmission-unconstrained deployment. This is because the solar field, which has a 2.0 SM, is oversized relative to the powerblock. Thus, it collects more energy than the powerblock

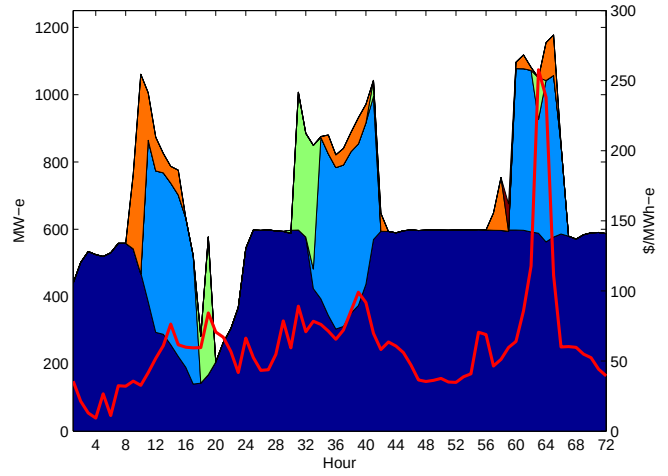

(a) Transmission-unconstrained.

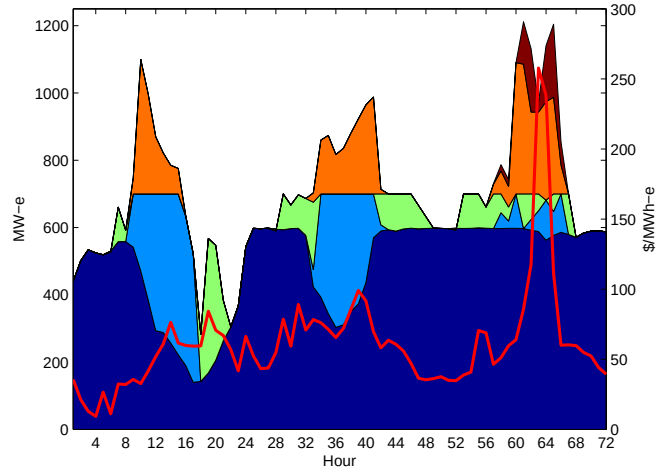

(b) Transmission-constrained.

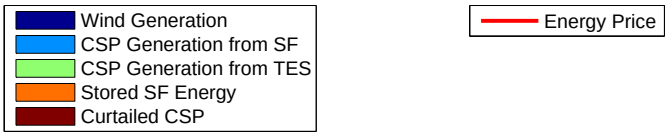

Fig. 4. Wind and CSP dispatch beginning 17 October, 2004. Fig. 4a shows transmission-unconstrained case, Fig. 4b shows transmission-constrained case.

can use. While some of this energy is stored, TES is energy-constrained resulting in about 2% of the 1115 GWh-t collected by each plant annually being curtailed. Thus, a wind-only deployment minimizes curtailment if the deployment is transmission-unconstrained. There is 3 GWh of curtailment in this case as well, however this is due to negative energy prices during a handful of hours. A mix of wind and CSP minimizes curtailment with constrained transmission, since the negative resource correlation results in fewer transmission constraint violations. With 600 MW and 800 MW of transmission 480 MW-e and 360 MW-e of CSP give minimum annual curtailments of 482 GWh and 192 GWh, respectively.

On the whole, CSP earns considerably higher energy revenues than wind. This is due to CSP having a slightly higher capacity factor and because CSP produces higher-value energy due to the coincidence between DNI and prices and the use

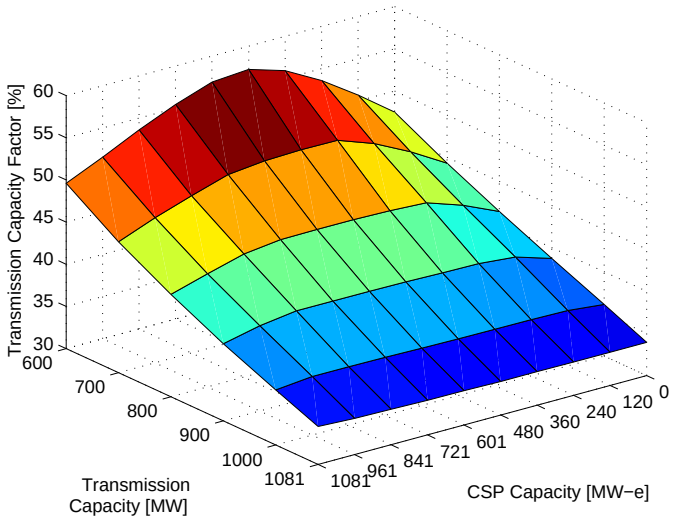

Fig. 5. Average annual transmission capacity factor.

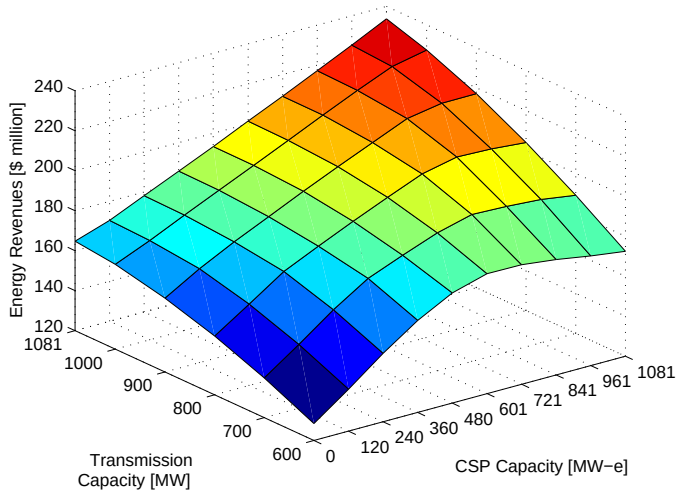

Fig. 7. Average annual energy revenues, excluding wind PTC.

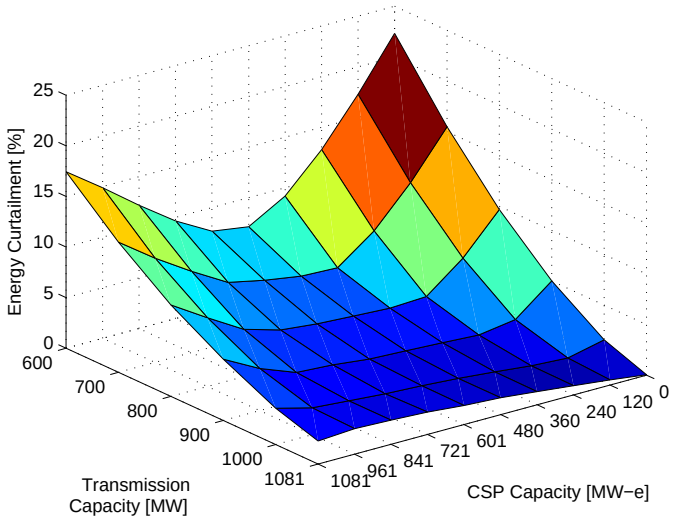

Fig. 6. Average annual energy curtailment.

of TES [12]. Thus, an all-CSP deployment gives maximum annual energy revenues of $234 million. Downsizing transmission significantly reduces revenues, with a much greater effect on CSP. Reducing the transmission capacity from 1080 MW to 600 MW reduces annual revenues of an all-CSP deployment by 26% or $61 million, as opposed to 22% or $36 million (excluding the PTC) for wind. The greater effect on CSP reflects the fact that much of CSP's value is from its ability to use TES to deliver energy during high-price hours, which is limited when transmission-constrained. With 600 MW and 800 MW of transmission 600 MW-e and 840 MW-e of CSP give maximum annual revenues of $180 million and $206 million, respectively.

B. Long-Term Economics of Co-Located Wind and CSP

Our analysis thus far assumes the deployment configuration and analyzes short-term operations. A related question is what deployment configuration maximizes long-term economic value. Such an analysis requires comparing upfront capital costs against discounted revenue streams over the deployment's lifetime, raising two challenges. One is that we only have two years of time-coincident wind and solar resource data. A second is that the cost of utility-scale CSP is uncertain due to commodity price fluctuations and the potential for manufacturing improvements. In light of these factors, we combine our revenue estimates with wind, CSP, and transmission cost forecasts to estimate a year-1 ROI. This ROI is defined as the fraction of deployment investment costs that are recovered through annual revenues. We now detail the revenue, cost, and subsidy assumptions underlying these calculations.

1) Deployment Revenues: The deployment is assumed to earn energy revenues net of variable costs, as defined by (1), and capacity payments, as detailed in section II-B.

2) Deployment Capital Costs: We account for the capital cost of wind, CSP, and transmission. We assume wind costs $1650/kW in 2006 dollars [29] and deflate this to $1598/kW in 2005 dollars using consumer price index data provided by the U.S. Department of Labor's Bureau of Labor Statistics. Turchi *et al.* [10] forecast 2020 CSP construction costs in 2010 dollars. We break these costs into three components—a solar field cost that is proportional to the plant's SM, a TES cost that is proportional to the hours of storage, and a fixed balance-of-plant cost, which includes the powerblock. The TES cost assumes that the power capacity is equal to the nameplate powerblock capacity, and does not account for the larger charging capacity that we use. If this larger charging capacity is used in the default system modeled in SAM, the TES cost increases by about 20%. Thus, we inflate the TES cost reported by Turchi *et al.* by 20% to arrive at the TES cost of the system that we model. Because of fluctuations in component costs, we deflate the costs reported in 2010 dollars to 2005 dollars using the Chemical Engineering Plant Cost Indices.[1] These calculations yield a solar field cost of $133 million/SM, a TES cost of $10.59 million/hour, and a balance-of-plant cost of $129.69 million.

[1]These indices are available online at http://www.che.com/pci/.

Analyzing AC and high-voltage DC transmission built between 1995 and 2008 reveals highly variable and possibly site-specific construction costs [3]. Nevertheless, most projects cost between \$200/km-MW and \$800/km-MW, and we use these as bounding values on the cost of transmission.

3) Deployment Subsidies: Our analysis focuses on Federal renewable subsidies. These include a \$19/MWh (in 2005) PTC for wind and a 30% investment tax credit (ITC) on the capital cost of solar. We assume that this ITC applies only to CSP plants, and excludes supplemental costs, such as transmission.

4) Deployment ROIs: We compute our ROIs as:

$$\frac{\chi^e + \chi^c + \chi^p}{\psi^w + (1 - \Upsilon^{ITC}) \cdot \psi^s + \psi^t}. \tag{24}$$

Deployments with an ROI at least as great as the CCR are said to be economic, since annual revenues are greater than the annualized investment cost. Fig. 8 shows the deployment ROIs as a function of the transmission and CSP capacity, which are given as a percentage of the 1080 MW-e generating capacity. Fig. 8a and 8b assume \$200/km-MW and \$800/km-MW transmission costs, respectively. Deployments that have an ROI of at least 11%, which is our assumed CCR, are denoted with magenta circles and the deployment with the highest ROI is denoted with a black cross.

Comparing Fig. 8a and 8b shows that deployment economics are highly sensitive to the transmission cost. There are no economic deployments if the cost of transmission is greater than about \$485/km-MW. However there are a number of deployment configurations with transmission capacities as low as 700 MW and up to 56% CSP on a capacity basis that are economic with a \$200/km-MW cost. Fig. 8b shows that the ROI-maximizing deployment with the higher transmission cost has a transmission link that is downsized relative to its generating capacity and is 22% CSP on a capacity basis, yielding an ROI of about 9.7%. While Fig. 8a suggests that wind-only deployments are optimal, this is partially due to the fixed CSP plant configuration considered. With a \$200/km-MW transmission cost, deployments including one CSP plant with a 1.0–1.9 SM, 1–4 hours of TES, and 900–1080 MW of transmission yield year-1 ROIs of 12%, which are comparable to the wind-only deployments shown. Moreover, the ROI-maximizing deployment with 600 MW and 800 MW of transmission are 33% and 22% CSP, respectively. Design flexibility improves CSP economics because the marginal value of increasing the plants' SM and hours of TES quickly diminish. Madaeni *et al*. [13] examine the overall economics of CSP, allowing for this design flexibility. They demonstrate that plants with SMs less than 1.8 and 3–4 hours of TES are economically robust, in that they achieve positive net year-1 ROIs in different electricity markets in the southwestern U.S. These results suggest that the baseline plant designs in the CSP literature are oversized, based on the what the market will bear.

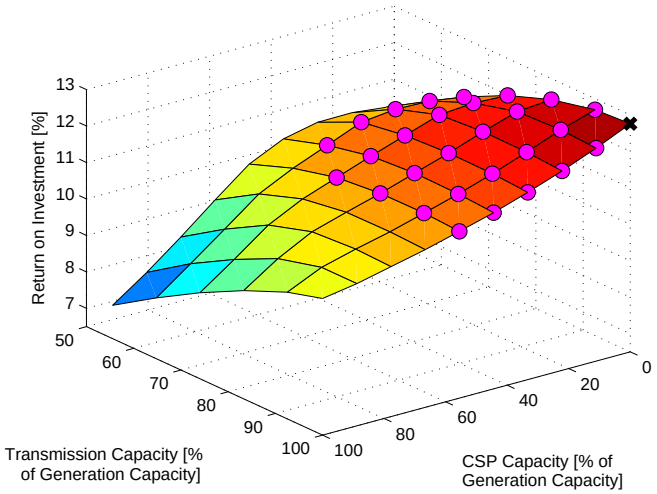

(a) \$200/km-MW transmission.

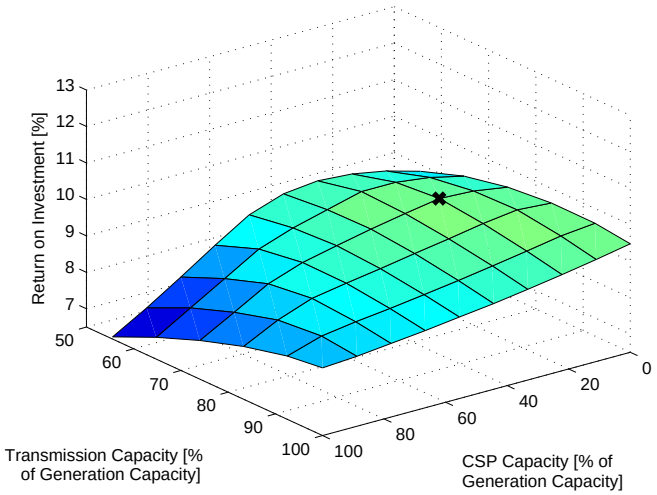

(b) \$800/km-MW transmission.

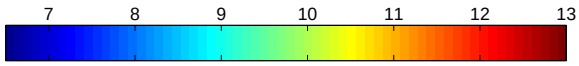

Fig. 8. Year-1 ROI. Transmission and generation capacities are given as a percentage of the 1080 MW-e generating capacity. Fig. 8a and 8b show \$200/km-MW and \$800/km-MW transmission cost cases, respectively.

IV. Conclusions

This paper analyzes the benefits of co-locating wind and solar generation in the southwestern U.S. Such a strategy improves the deployment's capacity factor, with TES shifting generation to lower-resource periods. However, adding transmission constraints reduces performance and the ability of CSP to provide maximum output during periods with high demand and wind. Even with TES, there are extended periods of high wind and solar resource, resulting in curtailment. Despite these limitations, we do find cases in which a mix of CSP and wind can be justified by market revenues. If the plants are flexibly configured, deployments with up to 67% CSP on a capacity basis yield a positive net ROI.

These findings depend on a reduction in CSP costs and deployment economics are sensitive to transmission costs, which have varied in the past. Turchi *et al*. [10] assume that CSP cost reductions come from the use of a molten salt HTF at a field temperature of 500° C, which is similar to a CSP configuration being tested by Enel at the 5 MW Archimede plant in Sicily, Italy. They further assume direct storage of the

HTF in a thermocline system [7], [30]. These improvements increase power cycle efficiency and lower TES cost. They also assume that advanced collector designs and manufacturing volume reduce solar field and other capital costs. Although we analyze Texas, there are many parts of the world that have co-located solar and wind resources for the type of deployments that we envision. This includes other parts of the southwestern U.S., northern Africa, the Arabian peninsula, the Tibetan plateau, northern Chile, and Australia. Our analysis determines what mixes of CSP, wind, and transmission are optimal based on long-term economics. One could, alternately, examine the economics of CSP using transmission already built for wind. This could be a useful exercise in Texas, which is currently investing in massive transmission projects to deliver wind to population centers [31]. Our analysis suggests that CSP could be economically built to exploit these assets and our model could be used to study these deployments in further detail.

Our analysis represents a snapshot of deployments in historic market conditions. Escalation in conventional generation costs, carbon restrictions, and other factors could increase the value of these deployments. While some of the value of dispatchable CSP is captured by the capacity payment, additional values of dispatchable energy, such as the provision of ancillary services, could increase revenues [12]. Finally, the value of dispatchable energy could change with increased penetrations of variable wind and photovoltaic solar.

Acknowledgment

The authors thank M. Mehos and C. Turchi for providing insights on CSP modeling, S. H. Madaeni for assistance with estimating LOLPs, and A. Lopez for generating the ERCOT resource map. R. Newmark, S. Succar, W. Short, T. Mai, and A. Sorooshian provided helpful comments and suggestions.

References

[1] *Study of Electric Transmission in Conjunction with Energy Storage Technology*, Lower Colorado River Authority, Austin, Texas, August 2003, prepared for Texas State Energy Conservation Office.

[2] R. Wiser and M. Bolinger, "2011 wind technologies market report," Lawrence Berkeley National Laboratory, Tech. Rep. LBNL-5559E, August 2012.

[3] P. Denholm and R. Sioshansi, "The value of compressed air energy storage with wind in transmission-constrained electric power systems," *Energy Policy*, vol. 37, pp. 3149–3158, August 2009.

[4] J. E. Pacheco and R. Gilbert, "Overview of recent results of the solar two test and evaluations program," Sandia National Laboratories, Tech. Rep. SAND99-0091C, January 1999.

[5] U. Herrmann and D. W. Kearney, "Survey of thermal energy storage for parabolic trough power plants," *Journal of Solar Energy Engineering*, vol. 124, pp. 145–152, May 2002.

[6] H. Price, E. Lüpfert, D. Kearney, E. Zarza, G. Cohen, R. Gee, and R. Mahoney, "Advances in parabolic trough solar power technology," *Journal of Solar Energy Engineering*, vol. 124, pp. 109–125, May 2002.

[7] J. E. Pacheco, S. K. Showalter, and W. J. Kolb, "Development of a molten-salt thermocline thermal storage system for parabolic trough plants," *Journal of Solar Energy Engineering*, vol. 124, pp. 153–159, May 2002.

[8] "Assessment of parabolic trough and power tower solar technology cost and performance forecasts," National Renewable Energy Laboratory, Tech. Rep. NREL/SR-550-34440, October 2003.

[9] D. W. Kearney, B. Kelly, U. Herrmann, R. Cable, J. E. Pacheco, A. R. Mahoney, H. Price, D. M. Blake, P. Nava, and N. Potrovitza, "Engineering aspects of a molten salt heat transfer fluid in a trough solar field," *Energy*, vol. 29, pp. 861–870, April-May 2004.

[10] C. Turchi, M. Mehos, C. K. Ho, and G. J. Kolb, "Current and Future Costs for Parabolic Trough and Power Tower Systems in the US Market," National Renewable Energy Laboratory, Tech. Rep. NREL/CP-5500-49303, October 2010.

[11] A. Gil, M. Medrano, I. Martorell, A. Lázaro, P. Dolado, B. Zalba, and L. F. Cabeza, "State of the art on high temperature thermal energy storage for power generation. part 1—concepts, materials and modellization," *Renewable and Sustainable Energy Reviews*, vol. 14, pp. 31–55, January 2010.

[12] R. Sioshansi and P. Denholm, "The value of concentrating solar power and thermal energy storage," *IEEE Transactions on Sustainable Energy*, vol. 1, pp. 173–183, October 2010.

[13] S. H. Madaeni, R. Sioshansi, and P. Denholm, "How thermal energy storage enhances the economic viability of concentrating solar power," *Proceeding of the IEEE*, vol. 100, pp. 335–347, February 2012.

[14] C. T. Wu, P. R. Shockley, and L. Engstrom, "The Intermountain Power Project 1600 MW HVDC transmission system," *IEEE Transactions on Power Delivery*, vol. 3, pp. 1249–1256, July 1988.

[15] P. Gilman, N. Blair, M. Mehos, C. B. Christensen, and S. Janzou, "Solar advisor model user guide for version 2.0," National Renewable Energy Laboratory, Tech. Rep. NREL/TP-670-43704, August 2008.

[16] A. Fiksel, J. W. Thornton, S. A. Klein, and W. A. Beckman, "Developments to the TRNSYS simulation program," *Journal of Solar Energy Engineering*, vol. 117, pp. 123–127, May 1995.

[17] H. Price, "Parabolic Trough Solar Power Plant Simulation Model," National Renewable Energy Laboratory, Tech. Rep. NREL/CP-550-33209, January 2003.

[18] M. R. Milligan and B. Parsons, "Comparison and case study of capacity credit algorithms for wind power plants," *Wind Engineering*, vol. 23, pp. 159–166, May 1999.

[19] M. R. Milligan and K. Porter, "The capacity value of wind in the united states: Methods and implementation," *The Electricity Journal*, vol. 19, pp. 91–99, March 2006.

[20] C. D'Annunzio and S. Santoso, "Noniterative method to approximate the effective load carrying capability of a wind plant," *IEEE Transactions on Energy Conversion*, vol. 23, pp. 544–550, June 2008.

[21] M. Amelin, "Comparison of Capacity Credit Calculation Methods for Conventional Power Plants and Wind Power," *IEEE Transactions on Power Systems*, vol. 24, pp. 685–691, May 2009.

[22] A. Keane, M. R. Milligan, C. J. Dent, B. Hasche, C. D'Annunzio, K. Dragoon, H. Holttinen, N. Samaan, L. Söder, and M. O'Malley, "Capacity Value of Wind Power," *IEEE Transactions on Power Systems*, vol. 26, pp. 564–572, May 2011.

[23] S. H. Madaeni, R. Sioshansi, and P. Denholm, "Estimating the Capacity Value of Concentrating Solar Power Plants: A Case Study of the Southwestern United States," *IEEE Transactions on Power Systems*, vol. 27, pp. 1116–1124, May 2012.

[24] ——, "Estimating the Capacity Value of Concentrating Solar Power Plants with Thermal Energy Storage: A Case Study of the Southwestern United States," *IEEE Transactions on Power Systems*, 2013, forthcoming.

[25] R. Billinton and R. N. Allan, *Reliability Evaluation of Power Systems*. Boston: Pitman Advanced Publishing Program, 1984.

[26] S. Wilcox, "National solar radiation database 1991-2005 update: User's manual," National Renewable Energy Laboratory, Tech. Rep. NREL/TP-581-41364, April 2007.

[27] C. W. Potter, D. Lew, J. McCaa, S. Cheng, S. Eichelberger, and E. Grimit, "Creating the Dataset for the Western Wind and Solar Integration Study (U.S.A.)," *Wind Engineering*, vol. 32, pp. 325–338, June 2008.

[28] R. Sioshansi, P. Denholm, T. Jenkin, and J. Weiss, "Estimating the value of electricity storage in PJM: Arbitrage and some welfare effects," *Energy Economics*, vol. 31, pp. 269–277, March 2009.

[29] "20% wind energy by 2030: Increasing wind energy's contribution to U.S. electricity supply," U.S. Department of Energy, Tech. Rep. DOE/GO-102008-2567, July 2008.

[30] G. J. Kolb, "Evaluation of Annual Performance of 2-Tank and Thermocline Thermal Storage Systems for Trough Plants," *Journal of Solar Energy Engineering*, vol. 133, August 2011.

[31] R. Sioshansi and D. Hurlbut, "Market protocols in ERCOT and their effect on wind generation," *Energy Policy*, vol. 38, pp. 3192–3197, July 2010.

Ramteen Sioshansi (M'11–SM'12) is an assistant professor in the Integrated Systems Engineering Department at The Ohio State University. His research focuses on renewable and sustainable energy system analysis and the design of restructured competitive electricity markets.

He holds a B.A. in economics and applied mathematics and an M.S. and Ph.D. in industrial engineering and operations research from the University of California, Berkeley, and an M.Sc. in econometrics and mathematical economics from The London School of Economics and Political Science.

Paul Denholm (M'11–SM'12) is a senior analyst in the Strategic Energy Analysis Center at the National Renewable Energy Laboratory. His research interests are in the effects of large-scale renewable energy deployment in electric power systems, and renewable energy enabling technologies such as energy storage and long distance transmission.

He holds a B.S. in physics from James Madison University, an M.S. in instrumentation physics from the University of Utah, and a Ph.D. in land resources/energy analysis and policy from the University of Wisconsin-Madison.